

# Tape cast porosity-graded piezoelectric ceramics

E. Mercadelli<sup>a,b,\*</sup>, A. Sanson<sup>a</sup>, P. Pinasco<sup>a</sup>, E. Roncari<sup>a</sup>, C. Galassi<sup>a</sup>

<sup>a</sup> Institute of Science and Technology for Ceramics, National Research Council, CNR-ISTEC, Via Granarolo 64, I-48018 Faenza, Italy

<sup>b</sup> Department of Industrial Chemistry and Materials, University of Bologna, Viale Risorgimento 4, I-40136 Bologna, Italy

Received 31 July 2009; received in revised form 10 November 2009; accepted 1 December 2009

Available online 19 January 2010

## Abstract

In this work a functionally graded porous Nb-doped PZT material (PZTN) was produced by tape casting. Each step of the production process (slurry formulation, lamination and thermal treatments) was thoroughly investigated. Tapes with different carbon black (CB) amounts were produced. The conditions necessary to laminate 6 layers of different CB concentration were optimized by tailoring the binder to plasticizer volume ratio of each single green layer. Cracks and delaminations were eliminated by gradually increasing CB content and adjusting the binder burn-out procedure. The optimization process led to a well developed, crack-free porosity-graded multilayer, less than 400  $\mu\text{m}$  thick and with porosity along the thickness ranging from 10 to 30 vol.%. The application of a load during the heating treatments was absolutely required to obtain warpage-free planar multilayer specimens.

© 2009 Elsevier Ltd. All rights reserved.

**Keywords:** FGM; Niobium doped PZT; Tape casting; Lamination; Porosity

## 1. Introduction

Porous piezoelectric materials are of great interest for ultrasonic applications ranging from hydrophones<sup>1,2</sup> to medical diagnostic devices.<sup>3</sup> In fact dense PZT-type piezoceramics are not appropriate for these applications due to their low hydrostatic figure of merit (FOM) (the product  $d_h g_h$ ). The stiff and dense PZT material has also the disadvantage of poor acoustic coupling to water or biological tissues. On the contrary, in porous piezoelectric materials, a partial decoupling between transverse and longitudinal effects leads a  $d_h$  increase. Moreover, due to the lower dielectric constant,  $g_h$  is further increased and consequently the hydrostatic FOM can reach values a few orders of magnitude higher than in dense materials.<sup>4</sup> A porous material however has a lower electromechanical coupling ( $k$ ) and piezoelectric charge ( $d$ ) coefficients in the thickness mode than those of the corresponding dense ones and therefore a lower piezoelectric response.

A porous Functionally Graded Material (FGM) allows to match the need of an high response, typical of dense piezoceramics, to a good compatibility with the investigated media given by a porous materials.

Porous graded piezoelectric materials more than 1 mm thick and with porosity ranging from 10 to 40% have been already produced by die-pressing.<sup>5–7</sup> With this technique it is however difficult to produce graded materials with thickness less than 1 mm. Reducing the material thickness let to reach higher resonance frequency and, as a consequence, high resolutions for reduced depth of field for transducers applications.<sup>8</sup>

Tape casting is the most used technique for the production of ceramic thin layers useful for graded materials less than 1 mm thick. Casting, lamination, debinding and sintering are necessary steps to obtain multilayers structure and any variation in these processes strongly affect the final product.

Mixing organic or inorganic pore-forming agents into a ceramic slurry before tape casting is considered an easy method for producing engineered porosity.<sup>9</sup> Carbon black (CB) is one of the most used pore-forming agents for its particles morphology and dimensions.<sup>10</sup>

The porosity gradient is formed *in situ* by sintering layer-stacked green tapes with stepwise varied contents of CB. Layers with different CB content show different shrinkage values that can cause delamination or warpage during sintering. These

\* Corresponding author at: Institute of Science and Technology for Ceramics, National Research Council, CNR-ISTEC, Via Granarolo 64, I-48018 Faenza, Italy. Tel.: +39 0546 699743; fax: +39 0546 46381.

E-mail address: [elisa.mercadelli@istec.cnr.it](mailto:elisa.mercadelli@istec.cnr.it) (E. Mercadelli).

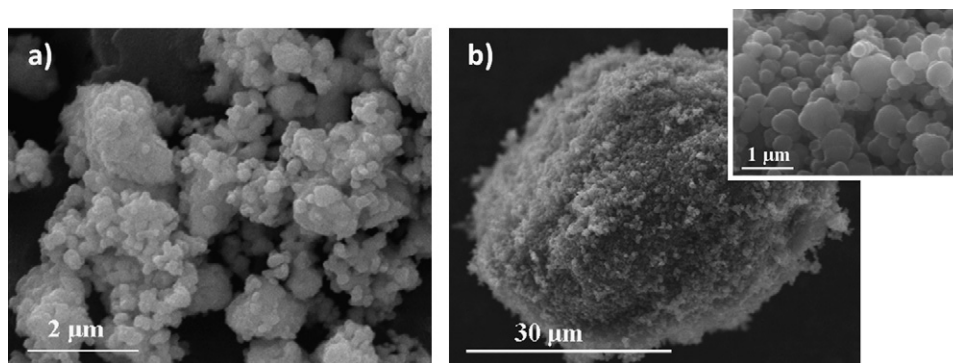


Fig. 1. SEM micrographs of the starting powders: (a) PZTN and (b) CB.

differences are reflected in strain rate mismatch and can be influenced by the layer thickness and viscosity ratio.<sup>11</sup> Applying pressure to the specimen during sintering (commonly indicated as constrained sintering) is a well known approach to avoid warpage.<sup>11–16</sup>

This paper thoroughly investigates the lamination and the thermal treatments needed to produce porous FGM of PZTN for ultrasonic applications. A planar crack-free FGM multilayer was obtained using constrained sintering. A porosity-graded, 400  $\mu\text{m}$  thick, PZTN multilayer with well developed and controlled microstructure, and porosity ranging from 10 to 30 vol.% was obtained and electrically characterized.

## 2. Experimental

PZTN powders [ $\text{Pb}_{0.988}(\text{Zr}_{0.52}\text{Ti}_{0.48})_{0.976}\text{Nb}_{0.024}\text{O}_3$ ] with average particle size of 0.6  $\mu\text{m}$  and specific surface area of 3.0  $\text{m}^2/\text{g}$  (BET Flowsorb II 2300 Micromeritics) were produced using the mixed oxides route. Carbon Black (CB, N99, Thermax-Cancarb), with average particle size of 1  $\mu\text{m}$  and specific surface area of 10.0  $\text{m}^2/\text{g}$ , was used as sacrificial pore-forming agent.

The layers with different CB amount (3, 9, 15, 20, 26, 33 vol.% respect to the PZTN powders) needed to obtain the FG piezoceramic were produced by tape casting. The slurries were prepared by adding to the starting ceramic powders the desired amounts of solvent (azeotropic mixture of ethyl alcohol and methyl ethyl ketone, Sigma–Aldrich), defloculants (a mixture of Butvar B98 and glycerine trioleate (GTO), Fluka), binder (Butvar B98, Monsanto Co., St Louis, MO, USA) and plasticizers (PEG 400, Fluka, and Santicizer 160 Monsanto Co., St Louis, MO, USA). The ball milled suspension was deaerated under vacuum and cast on a moving Mylar carrier ( $v = 6 \text{ mm/s}$ ) obtaining, after solvent evaporation, green tapes of  $100 \pm 10 \mu\text{m}$  thick.

The glass transition temperature ( $T_g$ ) of the green tapes was evaluated by differential scanning calorimetry (DSC) (Thermal Analyser Instruments Universal 2010 V4.4E). The analyses were performed between 20 and 100  $^\circ\text{C}$  at 10  $^\circ\text{C}/\text{min}$  heating rate.

An uniaxial warm press was used to laminate the green tape layers. Different layers with 40 mm diameter were stacked between two polished parallel steel plates and softened by heating for 30 min at temperature ranging from 40 to 60  $^\circ\text{C}$ . During

the thermal treatment a constant loading of 15 MPa was maintained. The lamination process was done with different tape orientations as top face to top face (t-t), top face to bottom face (t-b) and bottom face to bottom face (b-b). Tapes laminated in t-b configuration exhibit the most uniformity as compared to tapes laminated in t-t and b-b ones. This may arise because the presence of the smeared binder on the bottom surfaces is more available to uniformly block pores on the top surfaces for tapes laminated in t-b configuration.

The as-laminated samples were observed with an optical microscope (Leica DM RME) to verify the lamination results.

The debinding cycle was defined through thermo-gravimetric (TG) and DSC analyses carried out at 10  $^\circ\text{C}/\text{min}$  heating rate in a simultaneous thermal analyser (STA 449, Netzsch, Selb/Bavaria, Germany).

The single tapes were thermally treated at temperature between 900 and 1200  $^\circ\text{C}$  to find the best sintering conditions. The porosity of the sintered samples was evaluated by mercury intrusion technique (Pascal 140-240, Thermo Finnigan), by Archimedes' method and using an image analysis software (Image-Pro Plus) on SEM micrographs (SEM, Leica Cambridge Stereoscan 360).

Au electrodes were evaporated (automatic HR sputter coater, Assing) onto both sides of the samples for the electrical characterization. Samples were poled under applied fields of 3  $\text{kV}/\text{mm}$  at 120  $^\circ\text{C}$  for 40 min.

The piezoelectric properties of the porous graded multilayers were measured by a resonance-antiresonance method on the basis of IEEE 176-1987 standards, using an impedance analyzer (HP 4194A).

## 3. Results and discussion

### 3.1. Green tape

The SEM micrographs of the starting PZTN and CB powders are shown in Fig. 1. PZTN powder is formed by micrometric round agglomerates with primary particles size of about 0.25  $\mu\text{m}$ . On the other hand, the porous agglomerates of micrometric CB particles are easily broken down during the ball milling process leading to powders with a broad particle size distribution.<sup>10</sup>

Table 1  
Green tapes composition.

Tape	PZTN (vol.%)	Defloc. (vol.%)	Binder (vol.%)	Plast. (vol.%)	CB (vol.%)
3 <sup>a</sup>	43.72	4.95	37.23	12.75	1.35
9 <sup>a</sup>	39.49	4.48	37.36	14.72	3.95
15 <sup>a</sup>	35.71	4.05	37.47	16.47	6.30
20 <sup>a</sup>	32.69	3.70	37.54	17.90	8.17
26 <sup>a</sup>	29.32	3.33	37.64	19.45	10.26
33 <sup>a</sup>	25.29	2.87	37.77	21.46	12.61

<sup>a</sup> CB volume concentration referred to PZTN powder.

The green tape formulations with different CB amount (3, 9, 15, 20, 26, 33 vol.% respect to the PZTN powders) are reported in Table 1. According to Corbin et al.<sup>9</sup> an increase of the organic content (deflocculant, binder, plasticizers) was needed to counterbalance the introduction of CB in the suspensions and in order to obtain defect-free green tapes.

### 3.2. Lamination process

It is well known the critical role played by the lamination parameters in the manufacture of high quality multilayers.<sup>17</sup> Temperature ( $T_L$ ), pressure ( $P_L$ ), and time of lamination affect both strength and residual stresses in the laminates.

To optimize  $T_L$ , the stacked green layers with the 6 different CB content were laminated at temperature ranging from 40 to 70 °C, keeping constant pressure (15 MPa) and time (30 min). All the samples showed delaminations and/or squeezing defects (Fig. 2a) at each  $T_L$  investigated. This behaviour was attributed to the different organic composition of the tapes that influences the glass transition temperature ( $T_g$ ) of the binder.

The lamination process strongly depends on the green tapes properties, especially on the  $T_g$  of the binder-polymer. When the lamination temperature is sufficiently above the  $T_g$  of the binder ( $T_L - T_g \geq 50$  °C) the process depends mainly on the lamination time and pressure.<sup>17</sup> On the other hand, if the difference between the  $T_g$  of the binder and  $T_L$  is below 20 °C ( $T_g - T_L \leq 20$  °C) the lamination process is largely dependent on the lamination temperature only.<sup>18</sup>

In all the formulations considered the plasticizers are added to the binder to obtain a more flexible tapes at a given temperature. The plasticizer can modify the binder-polymer chain and therefore its  $T_g$  in two ways: (i) shortening the polymer chain length, (ii) partially dissolving it. With both these mechanisms the  $T_g$  decreases at increasing plasticizers amount, that is lowering the binder to plasticizer volume ratio ( $Y$ ) of the slurry composition.

To evaluate the influence of the  $T_g$  on the lamination temperature, it was important to know the  $T_g$  of each single tape forming the multilayer. The  $T_g$  value of pure binder (polyvinyl butyral) is 78 °C. The tape with lower CB concentration (3 vol.%) shows a quite different  $T_g$  in respect to the pure binder. For higher CB content more plasticizer was used causing a decrease in  $T_g$ . As reported in Fig. 3 tapes with different  $Y$  value show a quite different  $T_g$  value. As a result the stacked green sheets, having  $T_g$  ranging from 33 to 45 °C, cannot be successfully laminated. For example a lamination temperature of 40 °C is high enough to soften and laminate the green sheets with  $Y$  lower than 2.18, but insufficient to laminate the green sheets with higher  $Y$  values (Fig. 3). On the contrary working at 60 °C, an efficient lamination occurred among the layers with the highest  $Y$  values, but strong squeezing effect associated with deformation was caused in the green layers with the lowest  $Y$  value.

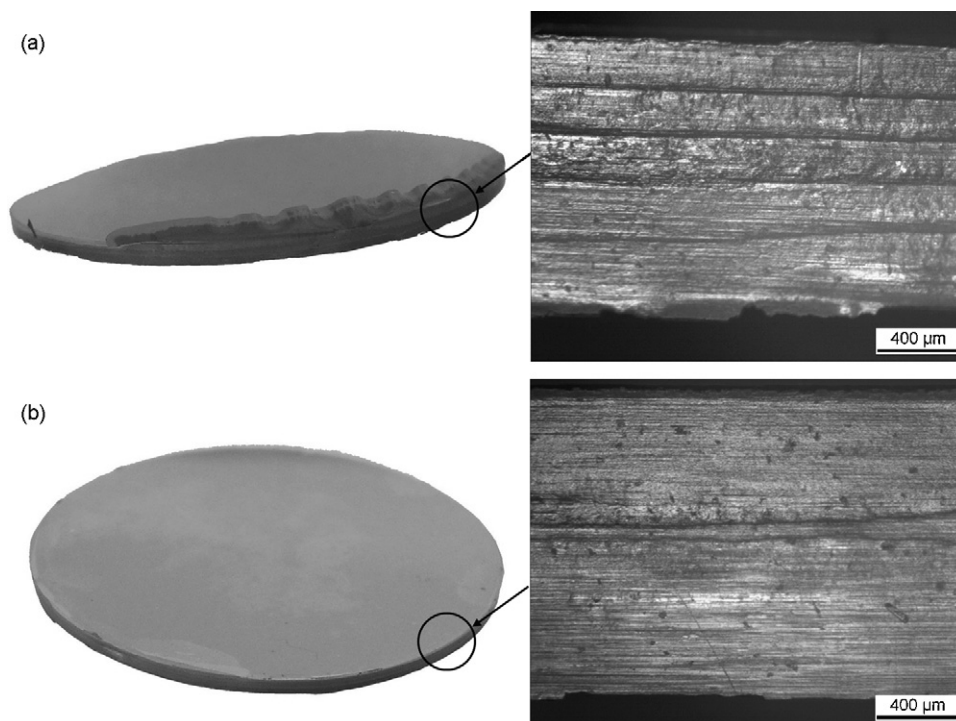


Fig. 2. Photo and optical micrograph of as-laminated ( $T_L = 60$  °C,  $P_L = 15$  MPa) FG multilayer with green sheets at different  $Y$ : (a)  $Y$  variable and (b)  $Y$  constant.

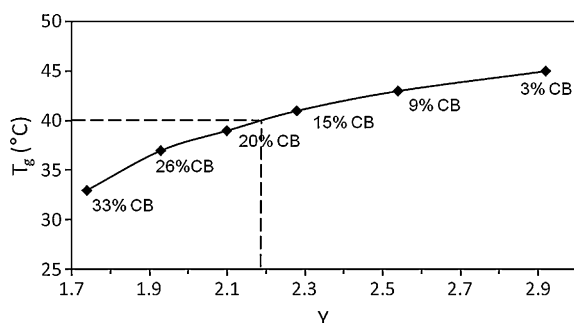


Fig. 3. Glass transition temperature of the green tapes with different CB content and Y ratio (Tapes Batch 1: variable Y).

For these reasons, new slurry compositions for each CB concentration were formulated by keeping the Y ratio constant. The slurries were formulated using the same binder amount of the previous Y variable-batch but gradually decreasing the plasticizers content to examine Y values from 1.7 to 3.0. 2.92 was considered the most suitable Y value for each composition. Higher values led in fact to rigid or even cracked green tapes, whereas for  $Y < 2.92$  an oily phase was detected on the surface of the tapes 7 days after the casting. This aging effect can be related to an excess of plasticizers trapped by the binder matrix during the casting process. This excess is then released as a consequence of a relaxation of the polymer network with time. Table 2 reports the binder and plasticizers amounts and their volume ratio Y for each batch.

The lamination process previously described was repeated with these new Y constant green tapes. Temperatures between 40 and 70 °C at constant loading (15 MPa) and time (30 min) were considered. It was found that 60 °C is the best temperature to obtain defect-free multilayers (Fig. 2b).

This study points out that the optimum laminating conditions are strongly dependent on the binder to plasticizers ratio (Y). For a successful lamination the stacked green sheets, in fact, must have the same  $T_g$  to allow an homogeneous softening of the structure and good interlayer adhesion without squeezing defects.

The lamination process produced a mean reduction of 7% in sample thickness in respect to the total thicknesses of the component green tapes that causes an increase of the bulk green density. It is well known<sup>19</sup> that the lamination process improves the effective packing density of the multilayer, inducing the deformation

necessary to promote adhesion between the layers only in the thickness direction while hindering it along X–Y. The bulk green density was geometrically calculated either for the single tapes and for the multilayers as the ratio of the measured volume and weight. Whereas the theoretical density was calculated considering the amount of organics and powders in each dry green tape (Table 1), assuming no void space and the complete solvent evaporation. The relative green density (expressed as percentage of the theoretical one) was  $90 \pm 3\%$  for each green tape and  $95 \pm 3\%$  for the multilayer produced with them. These values indicate that the lamination process lowers the residual porosity, i.e. increases the green density.

The porosity reduction caused by the lamination step must therefore be taken in account for the production of functionally graded materials with the desired characteristics, leading to values of final porosity lower than the ones of the corresponding single layers. To evaluate the porosity reduction induced by the lamination process 6 layers of each single composition were laminated at the above mentioned conditions, obtaining 6 new multilayers (“multi-bulks”). The effect of the lamination process on the final porosity of these sintered multi-bulks will be discussed in the following paragraph.

### 3.3. Debinding and sintering

To optimize debinding and sintering process, TG and DSC analyses were carried out for each layer with different CB concentration (0, 3, 15, 20, and 33 vol.%) and constant Y value.

TG analyses show that the organic (deflocculant, binder, plasticizers) and inorganic (CB) decomposition takes place at temperatures ranging between 200 and 550 °C. The burn-out of these additives involves several steps. The deflocculant evaporates completely at 80 °C,<sup>20</sup> but it is not detectable for its low amount. The binder-plasticizers decomposition/oxidation occurs in the temperature range 200–470 °C through two exothermic peaks.<sup>20,21</sup> In addition the DSC curves show a strong exothermic peak centred at about 500 °C attributed to the CB combustion. As the CB concentration increases the relative exothermic peak becomes wider and slightly shifted towards higher temperatures. This is probably due to the different amount of organics present in each green tape. The heat evolution during the plasticizers and binder oxidation induces the exothermic CB decomposition at temperature below the tabulated one.<sup>22</sup>

Table 2  
Binder and plasticizers amount, and Y values for the two green tapes batches.

CB <sup>a</sup> (vol.%)	Tapes Batch 1: variable Y					Tapes Batch 2: constant Y				
	Binder		Plasticizers		Y	Binder		Plasticizers		Y
	(wt%)	(vol.%)	(wt%)	(vol.%)		(wt%)	(vol.%)	(wt%)	(vol.%)	
3	7.2	12.71	2.52	4.35	2.92	7.2	12.71	2.5	4.35	2.92
9	7.6	12.80	3.06	5.05	2.54	7.6	12.82	2.7	4.39	2.92
15	8.0	12.88	3.57	5.66	2.28	8.0	12.90	2.8	4.41	2.92
20	8.3	12.94	4.02	6.17	2.10	8.3	12.97	2.9	4.44	2.92
26	8.7	13.01	4.56	6.72	1.93	8.7	13.05	3.0	4.46	2.92
33	9.2	13.38	5.42	7.69	1.74	9.2	13.14	3.2	4.51	2.92

<sup>a</sup> CB volume concentration referred to PZTN powder.



Table 3  
Influence of thickness and number of layers on a successful debinding.

No. layers	Single layer thickness (μm)	Total thickness <sup>a</sup> (μm)	Debinded sample
3	200 ± 10	600 ± 30	OK
3	300 ± 10	900 ± 30	Cracked
4	200 ± 10	800 ± 10	OK
4	300 ± 20	1200 ± 20	Cracked
5	200 ± 20	1000 ± 40	Cracked
6	70 ± 10	400 ± 20	OK
6	100 ± 10	600 ± 30	OK
6	200 ± 20	1200 ± 40	Cracked
6	350 ± 20	2100 ± 30	Cracked
4	200 ± 20	1400 ± 40	Cracked

<sup>a</sup> Thickness of the as-laminated green multilayers.

The higher is the organic/CB ratio, the lower would be the CB combustion temperature.

The TG curves show that the total weight loss of the tapes corresponds to the theoretical organic amount used in the tape formulations. All the binder, plasticizers, deflocculant and CB were therefore burnt out completely without leaving any residues at 600 °C. The burn-out cycle was then carried out slowly and in several steps up to 600 °C to avoid the multilayer cracking. The debinding cycle used was: 50 °C/h to 150 °C; 4 °C/h to 230 °C; 3 °C/h to 480 °C with holding time 1 h, and 3 °C/h to 600 °C, the furnace was then left to cool down to room temperature.

A successful debinding step was found to be strongly related to the final thickness either of multi-bulks or FGM laminates. Several combinations of thickness and number of layers were considered to evaluate the most affecting factor among total thickness of the multilayers, single layer thickness and number of layers (Table 3). Only samples with total thickness below the critical value of  $800 \pm 20$  μm were found to be crack-free. This effect is thought to be due to increased residual stresses in the interlayers regions.<sup>23</sup> Piezospectroscopic investigations will be conducted to better understand this phenomenon.

The densification behaviour of single tapes with the lowest (3%) and highest (33%) CB content was examined at different temperatures for dwelling time of 1 h. Fig. 4 shows that the amount of open porosity, measured by mercury intrusion

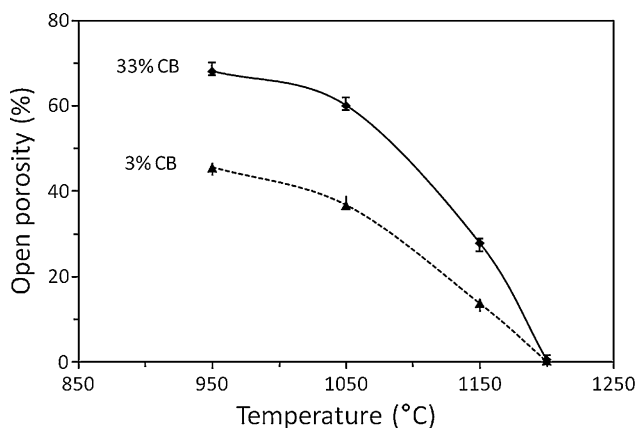


Fig. 4. Open porosity of sintered single tapes with 2 different CB concentrations as a function of the sintering temperature.

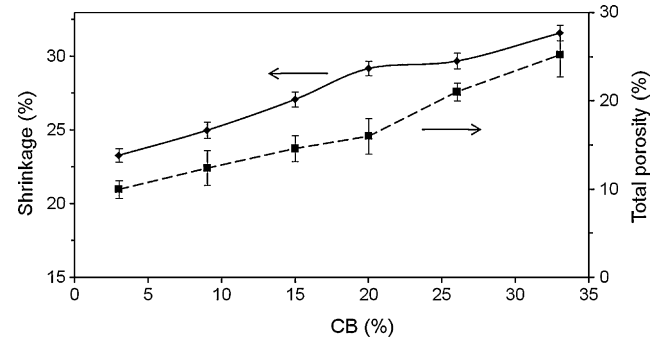


Fig. 5. Shrinkage and total porosity of the multi-bulks after sintering at 1150 °C for 1 h.

technique, is zero for temperatures higher than 1200 °C. The sintering process should enable the full densification of the layer with the lowest CB content retaining at the same time a good level of porosity in the other layers. As a consequence 1150 °C for 1 h was considered the best compromise in terms of porosity level and mechanical stability of the porous material.

As already mentioned, the lamination process induces a reduction of thickness that could be reflected in lower values of final porosity of the multi-bulks in comparison with the ones of the corresponding single tapes. For this reason, the total porosity and shrinkage were evaluated at 1150 °C for 1 h for each of the multi-bulk. Fig. 5 shows the total porosity of each multi-bulk, calculated by Archimedes' method, whereas in Fig. 4 is presented the open porosity, after sintering of the single layers with 3 and 33% of CB. The total porosity is usually defined as sum of the open and closed porosity, therefore the values presented in Fig. 5 should be higher than the ones of Fig. 4. On the contrary, the open porosity measured in the single layer is higher than the total one found in the correspondent multi-bulk confirming the porosity reduction induced by the lamination process.

The shrinkage (Fig. 5) ranges between 23% (multi-bulk with 3% of CB) and 32% (multi-bulk with 33% of CB). This high shrinkage difference between the two opposite layers forming the FGM led to sintered samples with severe distortions and warpage (Fig. 6a). A common method to limit warpage effects in multilayers is the application of a suitable load during sintering (constrained sintering). In this way it is possible to constrain the shrinkage in the thickness direction by hindering the one along the diameter and consequently preventing distortions and warpage in the sample. The samples were therefore placed between 2 flat zirconia substrates with loading pressure of 0.4 or 0.7 kPa.<sup>11</sup> The application of 0.4 kPa led to a warpage-free, 400 μm thick, planar FGM multilayer (Fig. 6b) whereas 0.7 kPa caused a severe cracking (Fig. 6c).

In the sintered FGM multilayer, no microstructural evidence of boundaries between the six original porous layers could be discerned (Fig. 7). The porosity calculated by image analysis of SEM micrographs ranges from 10 to 30%, whereas the mean grain size is about 2.5 μm.

The preliminary tests done on PZTN-FGM multilayer showed an acoustic impedance of  $15 \times 10^6$  kg/(m<sup>2</sup> s) and piezoelectric properties of  $S_{11}^E = 26 \times 10^{-12}$  m/N,  $k_p = 0.38$ ,

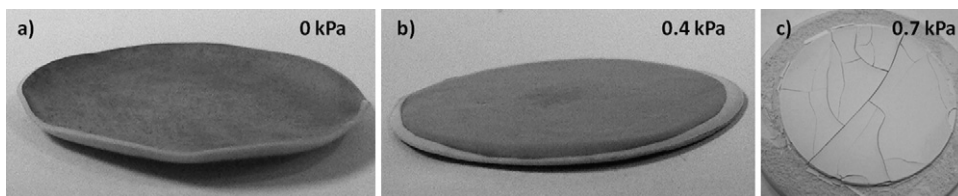


Fig. 6. FG multilayers constraint sintered by applying different loading pressure. Only the samples (a) and (b) shows Au electrode on the surface.

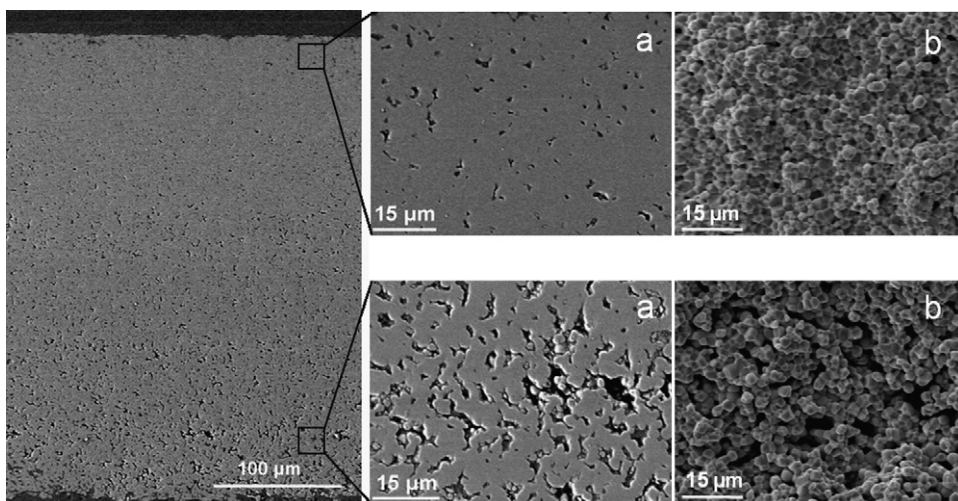


Fig. 7. SEM micrographs of the 6 layers porous graded PZTN material: (a) polished surface and (b) fracture surface.

$d_{31} = -106 \times 10^{-12}$  m/V. Those data confirmed the potentiality of this material for ultrasonic devices.

#### 4. Conclusions

The entire tape casting process was investigated and optimized to produce a functionally graded porous piezoelectric ceramic. This study showed that the lamination conditions can be optimized by tailoring the binder to plasticizer volume ratio ( $Y$ ) of each stacked green layer. Graded porous piezoceramics were fabricated by gradually increasing CB content, adjusting the binder burn-out procedure and tailoring the multilayer thickness. In this way cracks and delaminations were avoided, leading to a well developed and controlled microstructure with porosity ranging from 10 to 30 vol.%. A load applied during the heating treatments was required to obtain a warpage-free, 400 μm thick, planar multilayer specimen. The piezoelectric properties of these materials are suitable for ultrasonic applications.

#### Acknowledgment

We gratefully acknowledge Mr. F. Fochi for the electrical measurements.

#### References

- Boumchedda K, Hamadi M, Fantozzi G. Properties of a hydrophone produced with porous PZT ceramic. *J Eur Ceram Soc* 2007;**27**:4169–71.
- Marselli S, Pavia V, Galassi C, Roncari E, Craciun F, Guidarelli G. Porous piezoelectric ceramic hydrophone. *J Acoust Soc Am* 1999;**106**:733–8.
- Eremkin VV, Smotrakov VG, Aleshin VA, Tsikhotskii ES. Microstructure of porous piezoceramics for medical diagnostics. *Inorg Mater* 2004;**40**:775–9.
- Galassi C. Processing of porous ceramics: piezoelectric materials. *J Eur Ceram Soc* 2006;**26**:2951–8.
- Zhang HL, Li J, Zhang B. Microstructure and electrical properties of porous PZT ceramics derived from different pore-forming agents. *Acta Mater* 2007;**55**:171–81.
- Piazza D, Capiati C, Galassi C. Piezoceramic material with anisotropic graded porosity. *J Eur Ceram Soc* 2005;**25**:3075–8.
- Li J-F, Zhang H, Takagi K, Watanabe R. Porosity-graded piezoelectric ceramics: processing and electric-induced displacement. *Mater Sci Forum* 2005;**475–479**:1567–70.
- Opielinski KJ, Gudra T. Influence of the thickness of multilayer matching systems on the transfer function of ultrasonic airborne transducer. *Ultrasonics* 2002;**40**:465–9.
- Corbin SF, Lee J, Qiao X. Influence of green formulation and pyrolyzable particulates on the porous microstructure and sintering characteristics of tape cast ceramics. *J Am Ceram Soc* 2001;**84**:41–7.
- Sanson A, Pinasco P, Roncari E. Influence of pore formers on slurry composition and microstructure of tape cast supporting anodes for SOFCs. *J Eur Ceram Soc* 2008;**28**:1221–6.
- Lee SH, Messing GL, Awano M. Sintering arches for cosintering camber-free SOFC multilayers. *J Am Ceram Soc* 2008:421–7.
- Rishi, R., Co-fired Multilayer ceramic tapes that exhibit constrained sintering. United States Patent 5102720A, 7 April, 1992.
- Kodama, H., Okamoto, M., Suzuki, H., Ogihara, S., Moyoshi, T., Kobayashi, F., Method for producing multilayer ceramic body with convex side faces. United States Patent 5277720A, 11 January, 1994.
- Mikeska, K. R., Schaefer, D. T., Jensen, H., Method for reducing shrinkage during firing of green ceramic bodies. United States Patent 5085720A, 4 February, 1992.

15. Mikeska, K. R., Schaefer, D. T., Method for reducing shrinkage during firing of ceramic bodies. United States Patent 5254191A, 19 October, 1993.
16. Weinstein, R. N., Process for flattening alumina substrates. United States Patent 3792139A, 12 February, 1974.
17. Snel MD. Optimum lamination of ceramic green tapes. In: *Proceeding of 10th ECerS Conf.*. 2007. p. 457–60.
18. Yang TCK, Viswanath DS, Natarajan G. The effect of laminating factors on the thermal properties of unfired multilayer glass-ceramic and alumina substrates. *Polym Compos* 1997;**18**:539–46.
19. Sung JS, Koo KD, Park JH. Lamination and sintering shrinkage behaviour in multilayered ceramics. *J Am Ceram Soc* 1999;**82**:537–44.
20. Salam LA, Matthews RD, Robertson H. Pyrolysis of polyvinyl butyral (PVB) binder in thermoelectric green tapes. *J Eur Ceram Soc* 2000;**20**:1375–83.
21. Schultze D, Schiller WA. Burnout of organic components of glass ceramic composite tapes. *J Thermal Anal* 1998;**52**:211–9.
22. Cancarb-Thermax technical reference sheet.
23. Kiefer T, Moon H, Lange FF. Compressive surface layer to avoid edge cracking in laminar ceramic composite. *J Am Ceram Soc* 2005;**88**: 2855–8.